

## Analysis of a multiyear global vegetation leaf area index data set

Wolfgang Buermann,<sup>1</sup> Yujie Wang,<sup>1</sup> Jiarui Dong,<sup>1</sup> Liming Zhou,<sup>1</sup> Xubin Zeng,<sup>2</sup>  
Robert E. Dickinson,<sup>3</sup> Christopher S. Potter,<sup>4</sup> and Ranga B. Myneni<sup>1</sup>

Received 20 June 2001; revised 8 November 2001; accepted 6 December 2001; published 27 November 2002.

[1] The analysis of a global data set of monthly leaf area index (LAI), derived from satellite observations of normalized difference vegetation index (NDVI) for the period July 1981 to September 1994, is discussed in this paper. Validation of this retroactive, coarse resolution (8 km) global multiyear data set is a challenging task because repetitive ground measurements from all representative vegetation types are not available. Therefore the magnitudes and interannual variations in the derived LAI fields were assessed as follows. First, the use of a NDVI-based algorithm, as opposed to a more physically based approach, is estimated to result in relative errors in LAI of about 10–20%, which is comparable to the mean uncertainty of AVHRR NDVI data. Second, the satellite LAI values compared reasonably well to ground measurements from three field campaigns. Third, comparison with an existing multiyear LAI data set showed qualitative agreement with regards to interannual variability, although the LAI values of the earlier data were consistently larger than those derived here. Fourth, interannual variations in LAI were evaluated through correlations with climate data sets, e.g., sea surface temperatures and precipitation in tropical semiarid regions known for ENSO impacts, temperature dependence of vegetation growth, and therefore LAI, in the northern latitudes. The general consistency between these independent data sets imbues confidence in the LAI data set, at least for use in large-scale modeling studies. Finally, improvements in near-surface climate simulation are documented in a companion article when satellite LAI values were used in a global climate model. The data set is available to the community via our Web server (<http://cybele.bu.edu>). *INDEX TERMS:* 1640 Global Change: Remote sensing; 1620 Global Change: Climate dynamics (3309); 3322 Meteorology and Atmospheric Dynamics: Land/atmosphere interactions; *KEYWORDS:* NDVI, leaf area index, interannual variability, ENSO

**Citation:** Buermann, W., Y. Wang, J. Dong, L. Zhou, X. Zeng, R. E. Dickinson, C. S. Potter, and R. B. Myneni, Analysis of a multiyear global vegetation leaf area index data set, *J. Geophys. Res.*, 107(D22), 4646, doi:10.1029/2001JD000975, 2002.

### 1. Introduction

[2] The exchanges of energy, water, and carbon between the land and the atmosphere depends largely on the functioning of leaves. They use solar energy, water, atmospheric CO<sub>2</sub> and nutrients to synthesize sugars and other organic compounds. Stomates provide the path between the atmosphere and the water-saturated cellular tissues inside the leaves to facilitate the exchange of mass [Sellers *et al.*, 1997a]. Depending on environmental conditions, stomates act to optimize the uptake of atmospheric CO<sub>2</sub> and loss of water vapor, and, thus directly control evapotranspiration of

vegetated surfaces [Cowan, 1977; Field and Mooney, 1986]. Parameterizations for leaf functioning as part of climate models that simulate these processes require accurate quantitative information on the amount of vegetation [Dickinson, 1995]. In this context, the leaf area index (LAI) is one of the standard ecological parameters. It is defined as the one-sided green leaf area per unit ground area. In needleleaf vegetation, LAI is defined as the projected needleleaf area per unit ground area.

[3] LAI has been introduced in climate models to quantify water and carbon fluxes as well as the effect of leaves on the surface radiation balance [Dickinson, 1984]. One inconsistency in these efforts is that the model LAI values are often based on a few measurements from a less than ideal suite of sites that makes their extrapolation to other regions problematic. The availability of multiyear satellite data and recent advances in vegetation remote sensing provide an opportunity to overcome this deficiency. Several procedures have been developed to retrieve LAI from remotely sensed data. Empirical relationships between LAI and spectral vegetation indices, including near-infrared (NIR) to red (RED) band ratios and the normalized difference vegetation index (NDVI), have been suggested [Asrar

<sup>1</sup>Department of Geography, Boston University, Boston, Massachusetts, USA.

<sup>2</sup>Institute of Atmospheric Physics, University of Arizona, Tucson, Arizona, USA.

<sup>3</sup>School of Earth and Atmospheric Sciences, Georgia Institute of Technology, Atlanta, Georgia, USA.

<sup>4</sup>Ecosystem Science and Technology Branch, NASA Ames Research Center, Moffet Field, California, USA.

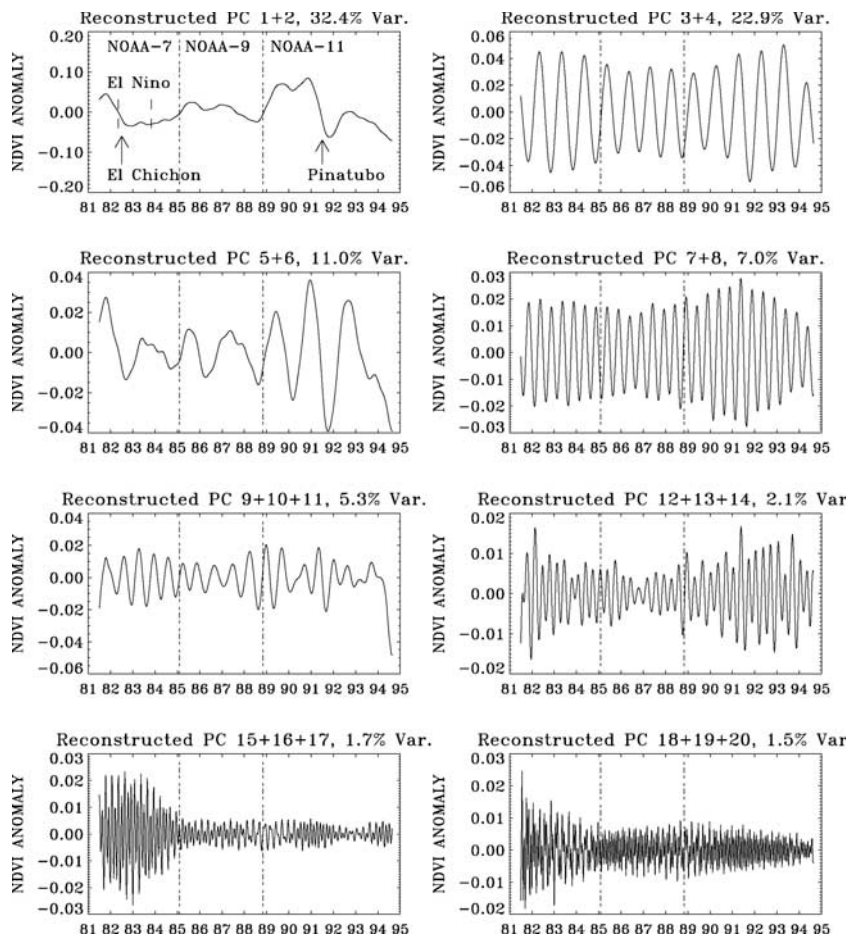


**Figure 1.** Singular spectrum analysis of the time series of five degree latitudinal band NDVI anomaly. The panel shows a selection of the first 20 reconstructed principal components from SSA analysis of the time series of spatially averaged PAL NDVI anomaly of vegetated pixels in the tropical band 5°S to 0°. Here, reconstructed principal components with similar spectral characteristics were grouped together. Window length was set to 90 (90 × 10 days ≈ 2.5 years) to primarily resolve periods at seasonal to interannual timescales [Vautard et al., 1992].

et al., 1984; Peterson et al., 1987; Chen and Cihlar, 1996; Sellers et al., 1996]. However, such relationships are site- and sensor-specific and their application to large areas or different seasons is limited [Gobron et al., 1997]. The preferred alternative for LAI retrievals from surface reflectances is a radiative transfer based approach that is accurate and applicable on an operational basis.

[4] In this paper, we present an analysis of a global monthly multiyear LAI data set for the period July 1981 to September 1994, derived from satellite NDVI with the aid of a three-dimensional radiative transfer model and a map of global land cover [Myneni et al., 1997a]. Establishing the validity of the produced LAI fields is a challenging task, yet without this, the utility of the data set for model studies of interannual variability in near-surface climate and terrestrial carbon cycle may be limited. Satellite data products are often validated with ground measurements, that is, an estimate of uncertainty of the produced fields is provided relative to some ground truth. The coarse spatial resolution of the LAI data set (8 × 8 km) and its global and temporal extent confound this task. Global validation requires field data from a range of sites representing a logical subset of the Earth’s land covers. Such activities

require significant resources and coordination. Moreover, the timeline of our data set implies dependence on past experimental campaigns.

[5] In spite of these limitations, we have tried nevertheless to assess the magnitudes and interannual variations in the produced LAI fields through five different activities. First, we perform an analysis to estimate the magnitude of errors incurred by the use of a NDVI-based algorithm as opposed to a radiative transfer based algorithm such as that used for the moderate resolution imaging spectroradiometer (MODIS). Second, ground measurements of LAI from three campaigns are used to verify the magnitude of the produced fields. Third, the data set is compared to another LAI data set currently used by the community. Fourth, through correlations with climate data sets, e.g., land and sea surface temperatures and precipitation, we argue for meaningful interannual variations observed in our LAI data set. Finally, the utility of the data set is documented through climate model simulations with the satellite LAI fields. This last activity is reported by Buermann et al. [2001]. While these activities do not constitute comprehensive validation per se, they do imbue sufficient confidence in the data set for further use and verification by the community.

## 2. Production of the LAI Data Set

[6] The NOAA/NASA Pathfinder AVHRR Land (PAL) data set consists of 10 day maximum NDVI value global composites for the period July 1981 to September 1994 [James and Kalluri, 1994]. The NDVI is expressed on a scale between  $-1$  to  $+1$ . It is between  $-0.2$  and  $0.1$  for snow, inland water bodies, deserts and exposed soils, and increases from about  $0.1$  to  $0.7$  for progressively increasing amounts of vegetation [Tucker *et al.*, 1986]. The NDVI data capture the contrast between red and near-infrared reflectance of vegetation that is indicative of the abundance and energy absorption by leaf pigments such as chlorophyll. The processing included improved navigation, calibration and partial atmospheric correction (Rayleigh scattering and ozone absorption) of the data. Remaining atmospheric effects were minimized by analyzing only the maximum NDVI value within each 10 day interval. However, residual noise due to orbital drift, intersensor variations and stratospheric aerosol effects in the data, have been reported [Myneni *et al.*, 1998]. Therefore the PAL NDVI data were corrected as follows.

[7] The time series of NDVI for barren and vegetated pixels in 5 degree latitude bands were extracted from a quarter degree NDVI data set, created by aggregating the 8 km data, using the land cover classification reported by Myneni *et al.* [1997a]. The spatial aggregation over the specific surface types emphasizes temporal variations in the NDVI fields that is the focus here. After subtracting the mean, based on the full record length, each of the resulting spatially averaged NDVI anomaly time series was subjected to singular spectrum analysis (SSA), which is a form of principal component analysis in the time domain [Vautard *et al.*, 1992]. The first 8 principal components (PCs) generally accounted for about 95% of the variance in the series. However, for the tropical bands significant high-frequency noise in the PAL NDVI data, likely due to residual cloud contamination, required inclusion of a larger number of PCs. For example, Figure 1 shows the first 20 reconstructed principal components for all vegetated pixels in the tropical band  $5^{\circ}\text{S}$  to  $0^{\circ}$ . The sum of the reconstructed PCs 3 and 4 shows the expected regularly recurring annual cycle corresponding to wet and dry periods. In contrast, the reconstructed PCs 1 and 2 as well as 5 and 6 capture the degradation due to stratospheric aerosols (Pinatubo, El Chichon), intersensor variations, and changes in overpass time and associated solar zenith angle effects resulting from orbital loss at the end of the satellites lifetime [Myneni *et al.*, 1998]. The effects of the seasonal movement of the ITCZ and related changes in atmospheric water vapor content on the NDVI data in this tropical band are likely to be captured in the sum of the reconstructed PCs 7 and 8 [Los *et al.*, 1994]. The remaining PCs explain only a small portion of the variances in the PAL NDVI data and mostly exhibit high-frequency variations from residual cloud contamination. The PAL NDVI anomaly time series for this tropical band and the aggregated reconstructed PCs denoting noise and signal are shown in Figure 2. The latitude and surface specific noise time series were then subtracted from the original quarter degree and 8 km time series of all pixels in that 5 degree latitude band. Note that the signal time series still shows a pronounced negative anomaly in the post Pinatubo period

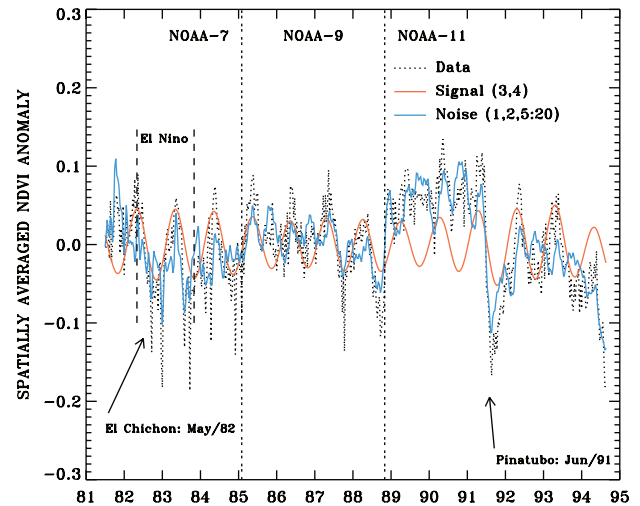


**Figure 2.** PAL 10 day NDVI anomaly time series (data) for vegetated pixels in the tropical band  $5^{\circ}\text{S}$  to  $0^{\circ}$  and aggregated principal components (PCs) denoting noise and signal. Numbers in brackets indicate the number of the PCs from Figure 1. The large-amplitude noise in these tropical vegetation data is due to residual cloud effects in the PAL NDVI data. Note also the impacts of stratospheric aerosols due to Mount Pinatubo eruption in June of 1991 and the dramatic loss of orbit in 1994.

(Figure 2). An evaluation of the corrected (noise-subtracted) NDVI time series confirms that for this period the data in the lower latitudes is still corrupted.

[8] The mean of the corrected three 10 day maximum NDVI value composites was used to create a monthly NDVI data set. Thereafter, this monthly NDVI data set was used to create the 8 km monthly LAI and Fraction of Absorbed Photosynthetically Active Radiation (FAPAR) data sets with an algorithm that utilizes results from a three-dimensional radiative transfer model and a land cover map as described by Myneni *et al.* [1997a].

### 2.1. Error Analysis

[9] We evaluated the magnitude of errors in the satellite LAI fields incurred due to uncertainties in input AVHRR NDVI data and deficiencies of the algorithm. The conversion of NDVI to LAI in the algorithm depends only on the vegetation type and measurement geometry, and this is also the principal deficiency [Myneni *et al.*, 1997a]. The NDVI is not a unique function of the component red and near-infrared channel reflectances. Thus, various combinations of the channel data can potentially result in the same value of NDVI, and hence, LAI. For example, consider two pixels of the same vegetation type but of different LAI values. The channel reflectances, even if measured under identical geometrical conditions, will be different, but may combine to result in similar NDVI, and hence LAI, values.

[10] To assess the magnitude of such errors, we use results from a recent effort in which the MODIS LAI algorithm and AVHRR based LASUR channel reflectances were utilized to retrieve LAI of broadleaf and needleleaf forests [Tian *et al.*, 2000; Berthelot *et al.*, 1997]. The NDVI based algorithm used here and the MODIS LAI algorithm

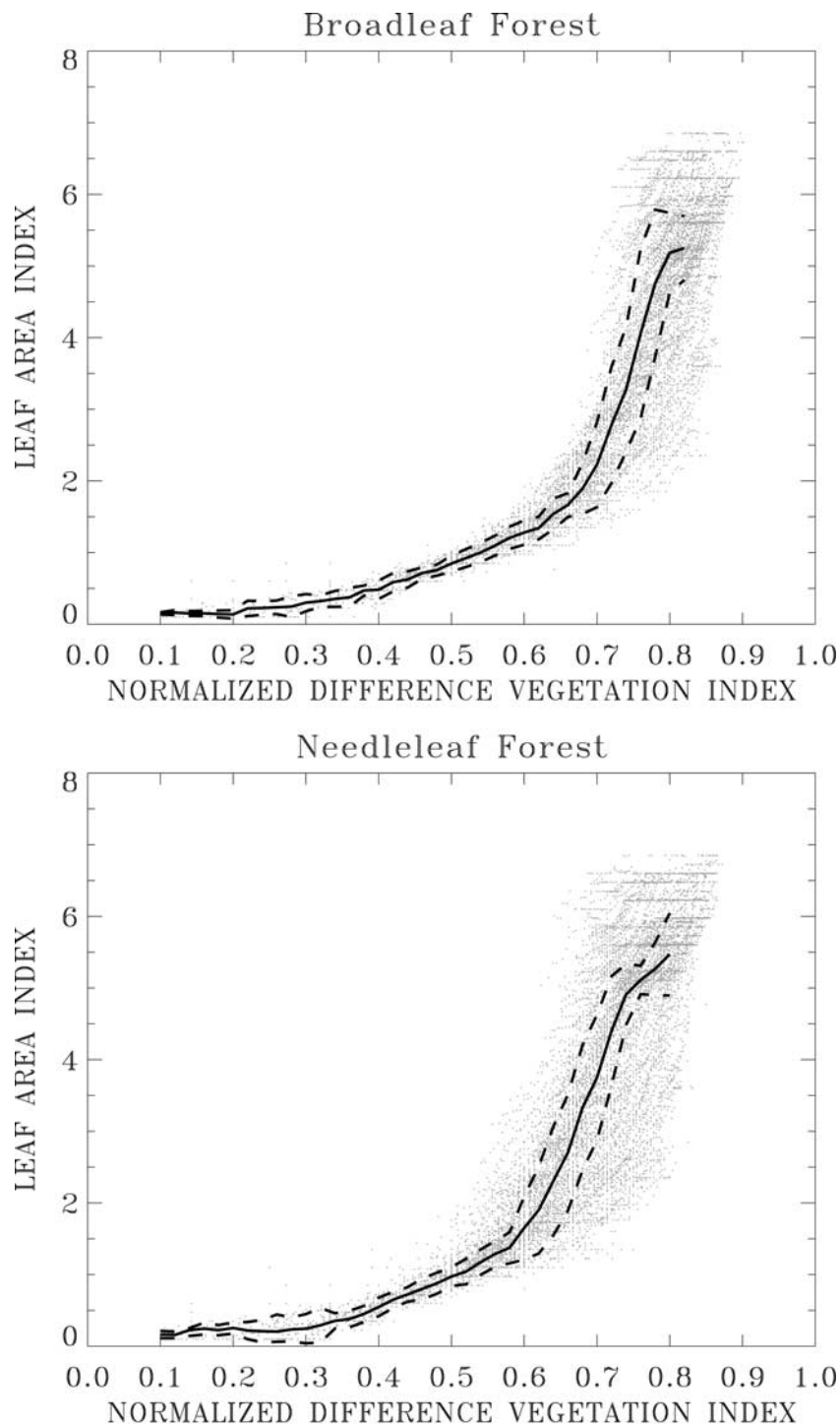


**Figure 3.** Scatterplot of the NDVI-LAI relationship for broadleaf and needleleaf canopies obtained from the MODIS algorithm using LASUR data [Berthelot *et al.*, 1997]. Solid lines are regression curves that represent the mean values of a Gaussian fit for each 0.02 NDVI interval. The regression curve is the best possible prediction of LAI and also minimizes the expected squared error of the prediction of LAI given a realized value of NDVI. The upper and lower sigma boundaries are shown as dashed lines.

are both based on the physics of radiative transfer. However, the MODIS algorithm ingests channel data, instead of NDVI, and also utilizes information on sun and view angles as well as background reflectances in the retrieval process [Knyazikhin *et al.*, 1998a]. Further, uncertainties in the input channel data are taken into account by the MODIS algo-

rithm through the use of a probabilistic approach that results in a LAI distribution function as the solution. LASUR reports no information on reflectance uncertainties. In such a case, it is necessary to identify at least the upper bound of the overall input channel uncertainty [Wang *et al.*, 2001]. One way to identify this upper bound is to set it to a fixed

**Table 1.** Mean and Standard Deviation of LAI at Specific NDVI Levels in Broadleaf and Needleleaf Forests, Using LASUR Data [Berthelot *et al.*, 1997] and the MODIS Algorithm [Knyazikhin *et al.*, 1998a]<sup>a</sup>

Biome	NDVI	LAI, $\mu$	Error, $\pm\sigma$
Broadleaf	0.5	0.85	0.11
	0.6	1.28	0.17
	0.7	2.23	0.59
Needleleaf	0.5	0.97	0.13
	0.6	1.65	0.44
	0.7	1.75	0.87

<sup>a</sup>For a given set of spectral reflectances, the MODIS algorithm produces multiple solutions of LAI which result from certain combinations of canopy/soil patterns leading to the same surface reflectance. In this algorithm, a mean uncertainty of 20% in the spectral surface reflectances is assumed [Tian *et al.*, 2000]. Analysis shows that the multiple LAI solutions are nearly normally distributed. The mean and standard deviation were obtained through a Gaussian fit and correspond to the conditional distribution of LAI in 0.02 NDVI intervals, centered at the respective NDVI values given in the table.

value and assess the performance of the algorithm on targets of known properties. For LASUR, an assumed overall input channel uncertainty of 20% indicated that 95% of the nonretrieved pixels were nonvegetated (NDVI < 0.1), and therefore this value was used in the retrieval process [Tian *et al.*, 2000].

[11] Figure 3 shows the conditional distribution of LAI with respect to NDVI evaluated from the red and near-infrared channel reflectances input to the MODIS algorithm. The scatter in the figure highlights the limitation of using a NDVI-LAI relation and, therefore, provides an estimate of errors incurred due to deficiencies of the NDVI-based algorithm.

[12] The results presented in Table 1 and Figure 3 indicate that in the NDVI range of 0.1 to 0.65 in broadleaf forests and 0.1 to 0.55 in needleleaf forests, relative errors in LAI are about 10–20%. This is approximately comparable to the overall uncertainty of input AVHRR channel data. The uncertainties in LAI grow for larger NDVI values, indicating retrievals from the saturation domain. Under such conditions, the canopy reflectances carry little signal for reliable LAI retrieval, because a wide range of natural variations in canopy structure and soil can result in the same value of the remotely sensed signal [Knyazikhin *et al.*, 1998b]. For the other four biomes (grasses, crops, shrubs and savannas) with relatively little or no tree fraction [Myneni *et al.*, 1997a], the frequency of LAI retrieval under saturation conditions is relatively low, thus minimizing this type of error. The errors in retrieved LAI values in these biomes are likely to be in the range of the uncertainties of the input data, about 20% [Tian *et al.*, 2000]. Errors in LAI retrievals due to biome misclassification are not considered here. Analysis presented in the work of Tian *et al.* [2000] indicates that misclassification of spectrally and structurally distinct biomes (e.g., grass and forests) can seriously degrade the quality of the retrieval.

### 3. Comparison With Field Observations

[13] The validation of coarse resolution global data sets with ground measurements is a difficult task. Here arises the challenging problem of scaling plot level measurements to satellite resolutions [Tian *et al.*, 2002]. The scarcity of field LAI measurements useful for validation during the 1980s

represents a more pressing problem. Nevertheless, we tried to utilize the few available LAI data from the following field campaigns (First International Field Experiment (FIFE), Oregon Transect Ecosystem Research (OTTER) and Boreal Ecosystem-Atmosphere Study (BOREAS)) as described below.

[14] A biome in a certain region at a given time has a LAI distribution that is dependent on the climatology and edaphic conditions [Potter *et al.*, 1993]. Sampling this distribution requires many plot-level, small-scale samples distributed over a large area which is expensive and not practical. Most field measurements are typically several plot level samples within a small region. Satellite retrievals, on the other hand, cover an entire region of interest, but at a coarse scale. If the sampling in both cases is adequate, the LAI distributions from field measurements and satellite data retrievals should approximate the true intrinsic distribution of the biome in that region at that time. By adequate we mean an optimum number of samples, but in practice we are limited to the available field data. Given a certain number of plot level measurements, we compare the resulting LAI distribution to that from coarse-scale satellite data retrievals for a biome in that region at about the same time period. If the two distributions are comparable, this then is the necessary, but not sufficient, condition for concluding that the distributions approach the true LAI distribution. It is not

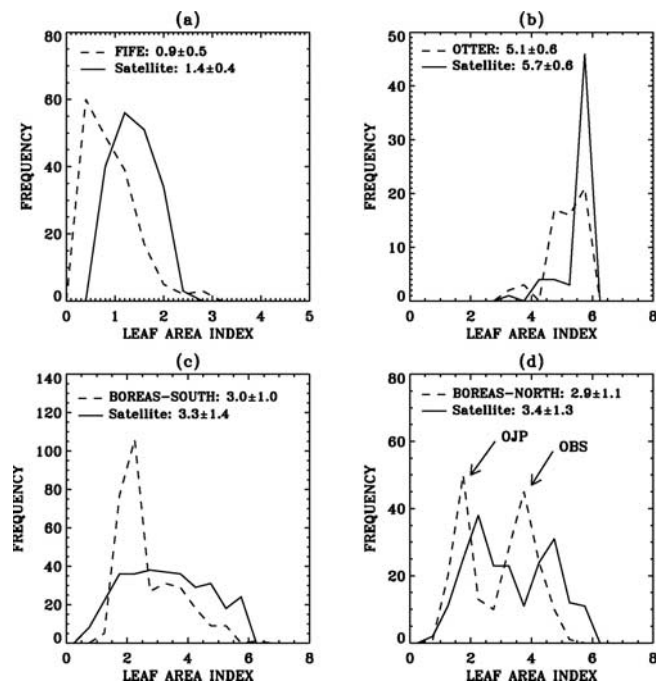


**Figure 4.** Comparison of field (dashed line) and 8 km satellite LAI (solid line) values for grasses and needleleaf forests. (a) FIFE (July 1987; 180 measurements), (b) OTTER (August 1990; 59 measurements), (c) BOREAS Southern Study Area (June 1994; 300 measurements) and (d) BOREAS Northern Study Area (June 1994; 200 measurements). The satellite LAI values are from 38.30°–39.70°N and 95.75°–97.25°W (FIFE), 44.40°–44.90°N and 122.10°–123.80°W (OTTER), 53.00°–54.50°N and 104.00°–106.50°W (BOREAS-SSA) and 55.00°–57.00°N and 96.50°–99.50°W (BOREAS-NSA), respectively.

**Table 2.** Differences in Mean Seasonal NDVI and LAI per Biome Between This Study and Those Reported by *Los et al.* [2000]<sup>a</sup>

Biome	Latitude	DJF		MAM		JJA		SON	
		$\Delta$ NDVI <sup>b</sup>	$\Delta$ LAI <sup>c</sup>	$\Delta$ NDVI	$\Delta$ LAI	$\Delta$ NDVI	$\Delta$ LAI	$\Delta$ NDVI	$\Delta$ LAI
Grasses	20°N–50°N	0.06	0.47	0.06	0.71	0.07	1.37	0.08	1.14
Shrubs	30°S–15°S	0.09	0.51	0.11	0.78	0.12	0.72	0.10	0.48
Broadleaf	40°N–55°N	0.10	0.43	0.07	0.65	0.06	1.90	0.10	1.11
Savannas	20°S–0°	0.06	1.27	0.06	1.07	0.08	1.02	0.13	0.84
Broadleaf	20°S–10°N	0.07	2.39	0.06	1.96	0.05	1.90	0.09	2.37
Needleleaf	50°N–65°N	0.07	0.36	0.06	0.17	0.09	1.29	0.04	1.22

<sup>a</sup>For this comparison, the monthly 8 km corrected Pathfinder NDVI and corresponding LAI data sets were aggregated to one degree spatial resolution, using an 8 km land cover map [*Myneni et al.*, 1997a]. The seasonal means of the NDVI and LAI fields are based on the time period of data record (January 1982 to December 1990). Spatial averaging for each biome and latitudinal band was performed over vegetated pixels (NDVI > 0.1 and LAI > 0), only.

<sup>b</sup>Difference between FASIR-NDVI [*Los et al.*, 2000] and this study.

<sup>c</sup>Difference between LAI from *Los et al.* [2000] and this study.

sufficient because the two sampled distributions may converge to the wrong distribution due to inadequate sampling. This is the logic behind our validation strategy.

[15] The FIFE experimental site is a  $15 \times 15$  km grassland area of the Konza Prairie in central Kansas, USA (39.00°N, 96.50°W). A total of 180 destructive grass samples at thirty plots were collected in July 1987. Subsequently, the leaf area of the grasses was measured with a LI-COR-3100 area meter [*Nelson et al.*, 1994]. These are compared to a similar number of 8 km satellite data LAI retrievals during the same period over grasslands in mid-western United States (Figure 4a). The distributions of field and satellite LAI values compare well, with the latter showing slightly higher LAI values. Apart from scaling issues, which perhaps explain some of this discrepancy, field retrievals possibly underestimate the actual LAIs due to rapid drying and change in shape of the grass samples [*Nelson et al.*, 1994].

[16] In the OTTER experiment, a total of 59 field photographic measurements were taken in August 1990 at two representative western coniferous sites in Oregon. The two sites are Warings Woods (44.60°N, 123.27°W; mountain hemlock and Douglas fir) and Scio (44.67°N, 122.61°W; mountain hemlock), at about 50 km apart. LAI values were computed from these photographic data [*Ustin*, 1990]. The resulting distribution is shown in Figure 4b together with the 8 km satellite data retrievals from needleleaf forests in this region during August 1990. The two distributions agree reasonably well and the most probable LAI value at these sites is about 5.5 to 6.

[17] A large number of overstory LAI measurements were made at several boreal conifer sites as part of the BOREAS experiment. These include old jack pine (OJP), old aspen (OA) and old black spruce (OBS). Most of these measurements were performed in June 1994 along transects at the intensive sampling sites (tower flux sites) located in the BOREAS southern study area (SSA) and northern study area (NSA), using a LI-COR LAI-2000 sensor [*Chen and Cihlar*, 1996]. About 300 measurements were made at three intensive sites (SSA-OA, SSA-OBS, and SSA-OJP) in the SSA, covering an area of about  $100 \times 50$  km. Likewise, about 200 measurements were made at two intensive sites (NSA-OBS and NSA-OJP) in the NSA, covering an area of  $40 \times 30$  km [*Chen and Cihlar*, 1996; *Sellers et al.*, 1997b]. We computed LAI values from these LAI-2000 readings, accounting for clumping effects as recommended by *Chen and Cihlar* [1996]. The resulting LAI distributions for the two study regions are shown in Figures 4c and 4d, together

with the 8 km satellite data retrievals from needleleaf forests in the boreal zone during June 1994.

[18] The field and satellite LAI distributions agree remarkably well at the NSA. The observed bimodality in the field data is due to a dense canopy at the OBS site ( $3.7 \pm 0.5$ ) and sparser canopy at the OJP ( $1.7 \pm 0.5$ ) site. The satellite data retrievals capture this, which also suggests that these two forest types are about equally common in that region. At the SSA, the satellite retrievals are generally higher than the field values. The distributions are also indicative of the different forest types. For example, the distinct peak at field LAI value of two is from OJP ( $1.9 \pm 0.2$ ) and OA ( $2.1 \pm 0.2$ ), while the shoulder at higher LAI values is due to OBS ( $3.4 \pm 0.2$ ). According to a land cover map of this region, high-density stands are more common at the SSA compared to the NSA [*Steyaert et al.*, 1997], but this is not reflected in the field LAI data. This possibly explains the discrepancy between the two distributions, in that the field samples at the SSA were not representative of the larger region. Moreover, all ground values at the BOREAS and OTTER sites represent overstory LAI only. The satellite retrievals include understory LAI as well [*Myneni et al.*, 1997a], which is an important part of the total LAI, especially in the boreal region, where the forest stands are often sparse and relatively open [*Chen and Cihlar*, 1996]. The measured NDVI of understory vegetation at BOREAS sites was reported to be about 0.35–0.50, the larger values at OBS sites [*Miller et al.*, 1997]. These NDVI values translate to an understory LAI of about 0.6 for OJP and about 1.0 for OBS sites [*Myneni et al.*, 1997a]. Accounting for the understory LAI reduces the discrepancy between the distributions shown in Figures 4b–4d.

[19] In summary, these results suggest that the magnitude of satellite LAI values are comparable to field observations, at select sites representative of grasses and needleleaf forest biomes. Similar exercises are required for the other biomes and obviously at many more sites. These activities are ongoing as part of MODIS LAI validation efforts [*Myneni et al.*, 2002].

#### 4. Comparison With Existing Data Sets

[20] A monthly LAI data set at one degree spatial resolution for the period January 1982 to December 1990 was developed by *Los et al.* [2000] from AVHRR NDVI data with corrections for satellite orbit loss, subpixel clouds and interpolation for missing data. The authors applied an empirical approach to derive LAI from FPAR-NDVI/SR

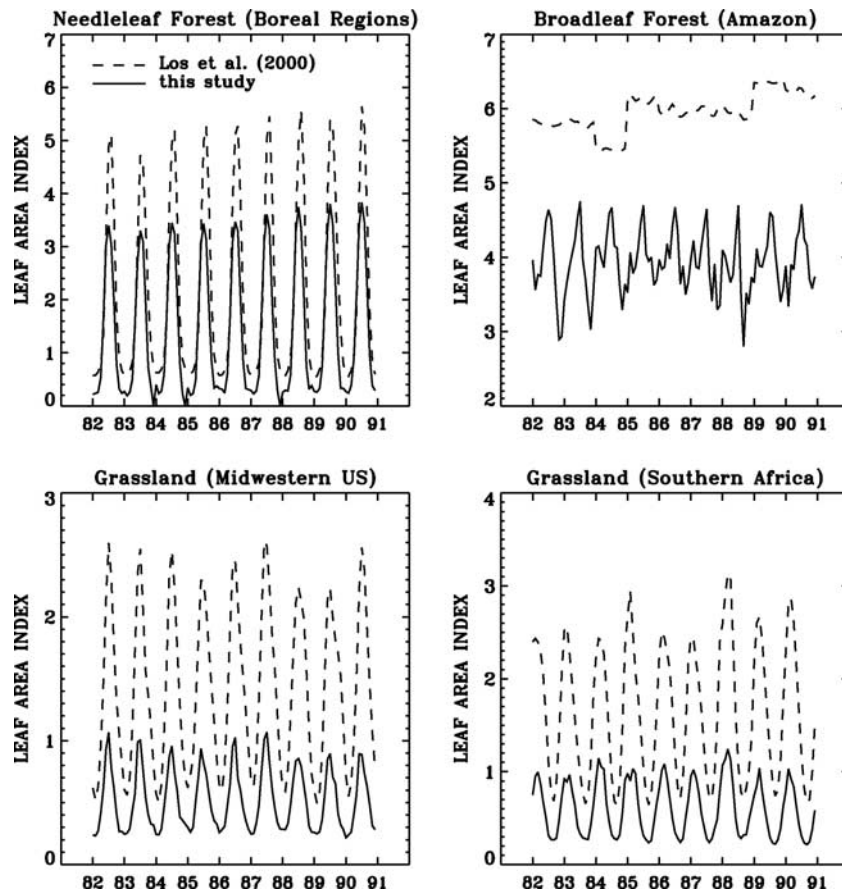


**Figure 5a.** Time series of spatially averaged monthly LAI from this study (solid line) and from *Los et al.* [2000] (dashed line) for selected regions. Spatial averaging for needleleaf forests was performed over all one degree pixels in the latitudinal band between  $50^{\circ}\text{N}$  and  $65^{\circ}\text{N}$ , for broadleaf forests from  $20^{\circ}\text{S}$  to  $10^{\circ}\text{N}$  and from  $40^{\circ}\text{W}$  to  $80^{\circ}\text{W}$ , for southern Africa grasslands from  $50^{\circ}\text{S}$  to  $0^{\circ}$  and from  $0^{\circ}$  to  $40^{\circ}\text{E}$ , and for midwestern U.S. grasslands from  $20^{\circ}\text{N}$  to  $50^{\circ}\text{N}$  and from  $60^{\circ}\text{W}$  to  $120^{\circ}\text{W}$ .

relationships based on work by *Sellers et al.* [1996]. We aggregated our 8 km LAI data, using a biome map [*Myneni et al.*, 1997a], to one degree resolution to enable a comparison of the two data sets.

[21] The LAI values from *Los et al.* [2000] are larger than our values in all biomes (Table 2 and Figure 5a). One reason for this consistent discrepancy is that the magnitudes of FASIR-NDVI for all biomes are also consistently larger compared to the corrected Pathfinder NDVI used in this study (Table 2). Most of these biases in NDVI is likely to be explained by differences in temporal compositing, *Los et al.* [1994] assign the maximum of all daily images within a monthly period to the monthly value, and a small reduction in the magnitudes of the Pathfinder NDVI data due to SSA corrections (see above). Further, *Los et al.* [2000] utilized the NDVI-LAI relational parameters that were derived at fine scales, to a relatively coarse scale. However, recent results from LAI retrieval efforts at multiple resolutions document the strong dependence of the NDVI-LAI relation on spatial scale [*Tian et al.*, 2002]. Generally, LAI values decrease with larger pixel sizes due to inevitable averaging over nonvegetated areas. The decrease of LAI with increasing area implies that application to coarser scales of fine scale derived NDVI-LAI relational parameters may result in significant LAI overestimates.

[22] A meaningful comparison between the LAI estimates from *Los et al.* [2000] and the biome specific field measurements presented previously is seriously compromised by the differences in spatial scales. Uncertainties resulting from mixing of different land covers and from the fact that the LAI magnitudes in general decrease with decreasing resolution due to averaging over nonvegetated areas are proportional to the differences in spatial scale under consideration [*Tian et al.*, 2002]. However, for completeness we extracted a few pixels from the one degree LAI fields of *Los et al.* [2000] and from the aggregated one degree LAI fields of this study over the corresponding field campaign sites. The results of this exercise yielded mean LAIs of  $4.1 \pm 1.0$  (Los) and  $2.1 \pm 1.1$  (this study) for FIFE ( $38.3^{\circ}$ – $39.7^{\circ}\text{N}$  and  $95.5^{\circ}$ – $97.5^{\circ}\text{W}$ ; 5 pixels),  $4.7 \pm 1.4$  (Los) and  $4.0 \pm 1.4$  (this study) for OTTER ( $44.0^{\circ}$ – $45.0^{\circ}\text{N}$  and  $121.5^{\circ}$ – $124.5^{\circ}\text{W}$ ; 3 pixels),  $3.4 \pm 0.2$  (Los) and  $3.4 \pm 0.3$  (this study) for BOREAS-SSA ( $53.0^{\circ}$ – $54.5^{\circ}\text{N}$  and  $104.0^{\circ}$ – $106.5^{\circ}\text{W}$ ; 6 pixels), and  $2.9 \pm 0.2$  (Los) and  $2.6 \pm 0.2$  (this study) for BOREAS-NSA ( $54.0^{\circ}$ – $58.0^{\circ}\text{N}$  and  $95.5^{\circ}$ – $100.5^{\circ}\text{W}$ ). For BOREAS, the LAI values from *Los et al.* [2000] represent the climatological mean based on the 9 year satellite record, since the field measurements and satellite observations do not timely overlap. In view of these and results from the previous section, and also from recent MODIS validation

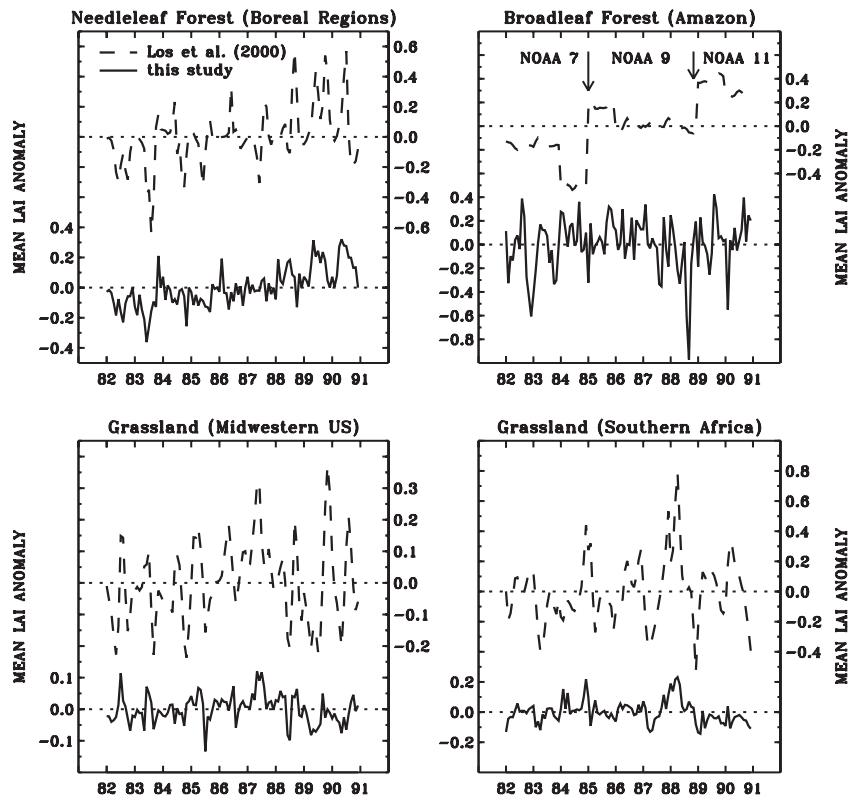


**Figure 5b.** Time series of spatially averaged monthly LAI anomalies from this study (solid line) and from *Los et al.* [2000] (dashed line) for the same regions as in Figure 5a. Anomalies were derived by subtracting the monthly pixel data from the 9 year (1982–1990) monthly mean values.

efforts reported by *Myneni et al.* [2002], it appears that the LAI values of *Los et al.* [2000] are overestimates in the case of grass canopies.

[23] The intra and interannual variations in LAI anomalies between the two data sets are qualitatively comparable in the case of needleleaf forest and grassland sites (Figure 5b). Our Amazonia LAI anomaly time series shows significant interannual variations, but some of this could be noise due to residual cloud contamination in the NDVI data set. To alleviate this problem, *Los et al.* [2000] utilized the annual maximum to represent data for all 12 months of the year. Their anomaly time series also shows artifacts related to change in satellites, possibly indicating an intersensor calibration problem.

[24] The use of our LAI data reduced some of the known cold biases in a recent global climate model study, resulting in better agreement between the simulated climate and observations of temperature and precipitation [*Buermann et al.*, 2001]. The simulations over grasslands were especially improved due to lower values of satellite LAI, relative to the standard values used in the model. The latter are comparable to the LAI magnitudes seen in the work of *Los et al.* [2000]. The lower satellite LAI values reduced land surface evapotranspiration, and consequently, enhanced sensible heat fluxes and near-surface air temperatures.

[25] In summary, the comparison of the two data sets indicated qualitative agreement with regards to interannual variability. However, it also showed that the LAI values of *Los et al.* [2000] were consistently larger than those derived

here. This highlights the importance of verifying satellite data products with ground measurements. We argue in favor of our data set in view of reasonable agreement with field data and improved simulation results from a global climate model using our data.

## 5. Comparison With Climate Variables

[26] The verification of satellite data LAI retrievals with ground measurements sampled from representative biomes and repeated in time is the preferred method of choice, but the scarcity of such measurements precludes this option. The dependence of vegetation growth on temperature and precipitation provides an alternative method in that spatial and temporal variations can be assessed for consistency with changes observed in meteorological fields. *Myneni et al.* [1996] have shown the interannual variation of NDVI and its association with tropical SST and other meteorological fields. Here we intend to use the same approach to evaluate the interannual variations in LAI with respect to anomalies in sea surface temperature, precipitation, and near-surface air temperature. To facilitate this analysis, the 8 km native data set was aggregated to a quarter degree resolution.

### 5.1. Spatial Averages of LAI and LAI Anomaly

[27] The time series of spatially averaged monthly LAI in broad latitudinal bands and globally are shown in Figure 6a. The averaging was done over vegetated areas only. The data

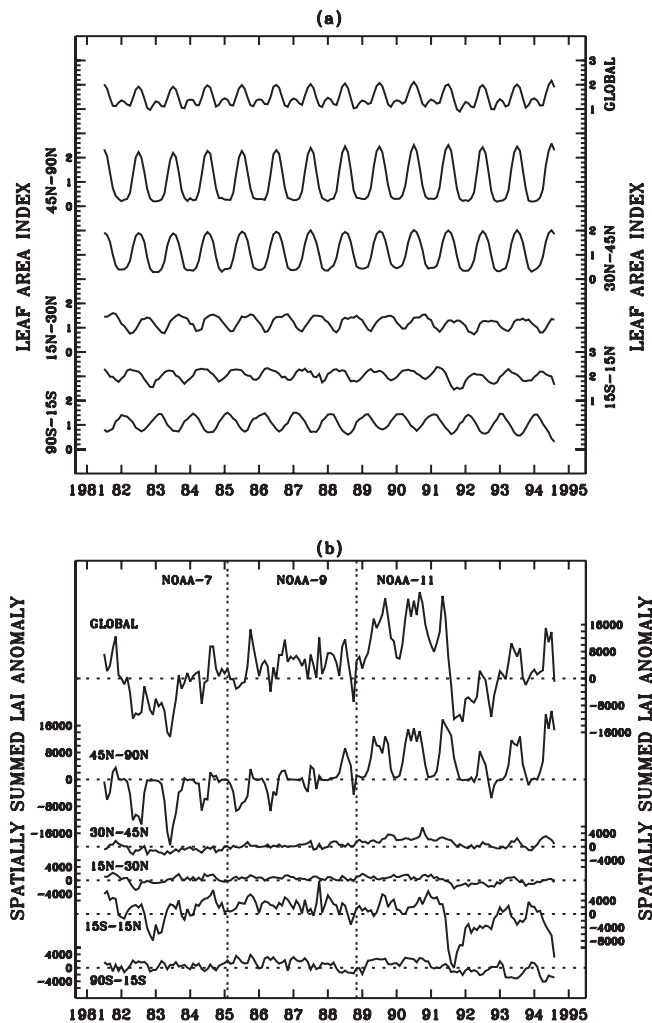


**Figure 6.** (a) Time series of spatially averaged monthly LAI for different broad latitudinal bands and the whole globe. (b) Time series of spatially summed LAI anomaly for different broad latitudinal bands and the whole globe.

clearly show the seasonality in the temperate and northern latitudes. The winter time LAI is close to zero at latitudes north of  $45^{\circ}\text{N}$ , largely due to lack of valid winter time data and low sun angles. The LAI values in the southern hemisphere show the opposite seasonality, with maximum LAI during the months of January and February. A gradual increase in boreal summer time LAI values in the northern latitudes can be seen, which was reported previously by *Myneni et al.* [1997b] from analysis of NDVI data during the 1980s.

[28] Monthly LAI anomalies were computed by subtracting the thirteen-year pixel monthly mean values (July 1981 to June 1994) from the pixel data. The time series of spatially summed LAI anomaly in broad latitudinal bands and globally are shown in Figure 6b. Spatially summed LAI anomalies, as opposed to spatial averages, correctly reflect the changing pixel numbers, i.e., seasonality, and thus are more informative. Further, this allows comparison of the contribution of each latitudinal band to the global LAI anomaly. The results of Figure 6b indicate that the global LAI anomaly pattern is dominated by northern vegetation

dynamics and to a lesser extent by variations in the tropics. The increasing trend in the northern high-latitude monthly LAI anomalies is also evident. The global anomaly time series shows a distinct period of negative LAI anomalies that coincides with the strong 1982–1983 ENSO event and the eruption of El Chichon (April 1982).

[29] The abrupt negative global anomalies over several months following the Pinatubo eruption (June 1991) are largely due to contributions from the tropics where the data were still deemed to be of poor quality (see above). The analysis in the following two sections is therefore restricted to the period July 1981 to June 1991, as the spatial scale of interest involves the entire globe.

## 5.2. Spatial Distribution of LAI

[30] The quarter degree LAI values were averaged over the 10-year period (July 1981 to June 1991) to obtain long-term, climatological, monthly LAI values. These monthly values were then further annually averaged with missing data given a LAI value of 0. Figure 7a shows the geographical distribution of the resulting annual LAI data. As expected, tropical evergreen forests have high LAI values, somewhat less green are the midlatitude broadleaf forests (e.g., eastern United States). Regions of low annual LAI values generally coincide with the global distribution of grasses and shrubs [*Myneni et al.*, 1997a]. The low LAI values of needleleaf forests in the boreal and temperate zones are largely an artifact associated with the lack of valid winter time data in these regions.

[31] Figures 7b and 7c show the geographical distribution of maximum and minimum LAI over the same 10-year period during the month of peak greenness. The latter was determined as the month of peak LAI from the climatological record. The LAI differences between the maximum and minimum values are large and seen notably in the forests of eastern United States, eastern China, central Africa, South America, and eastern Australia. Large relative LAI differences are seen in the grasslands of northeastern Brazil, southeastern South America, southern and eastern Africa, eastern Australia, the midwestern United States, southern Russia, and partly over northern high-latitude shrub lands.

## 5.3. LAI Variations Related to ENSO

[32] Several studies have focused on the relation between rainfall anomalies in the tropical continents and ENSO [*McBride and Nicholls*, 1983; *Ropelewski and Halpert*, 1987, 1989; *Dai et al.*, 1997; *Dai and Wigley*, 2000]. The shifts in convergence zones associated with ENSO have consequences for vegetation growth in the tropical arid and semiarid areas [*Myneni et al.*, 1996]. Two strong ENSO events occurred during the 1980s: the warm event of 1982–1983 and the cold event of 1988–1989, as evidenced from sea surface temperature (SST) anomalies in the equatorial tropical Pacific Ocean [*Reynolds and Smith*, 1994]. The time periods May 1982 to April 1983 (warm event) and May 1988 to April 1989 (cold event) were considered to examine the effects of ENSO related variations in the LAI data. Monthly LAI anomalies, relative to the ten-year monthly mean (July 1981 to June 1991), were summed and correlated with the NINO3 index (SST anomaly from the  $5^{\circ}\text{S}$ – $5^{\circ}\text{N}$  and  $90^{\circ}\text{W}$ – $150^{\circ}\text{W}$  region in the equatorial tropical Pacific) over the respective 12 month ENSO cycles.

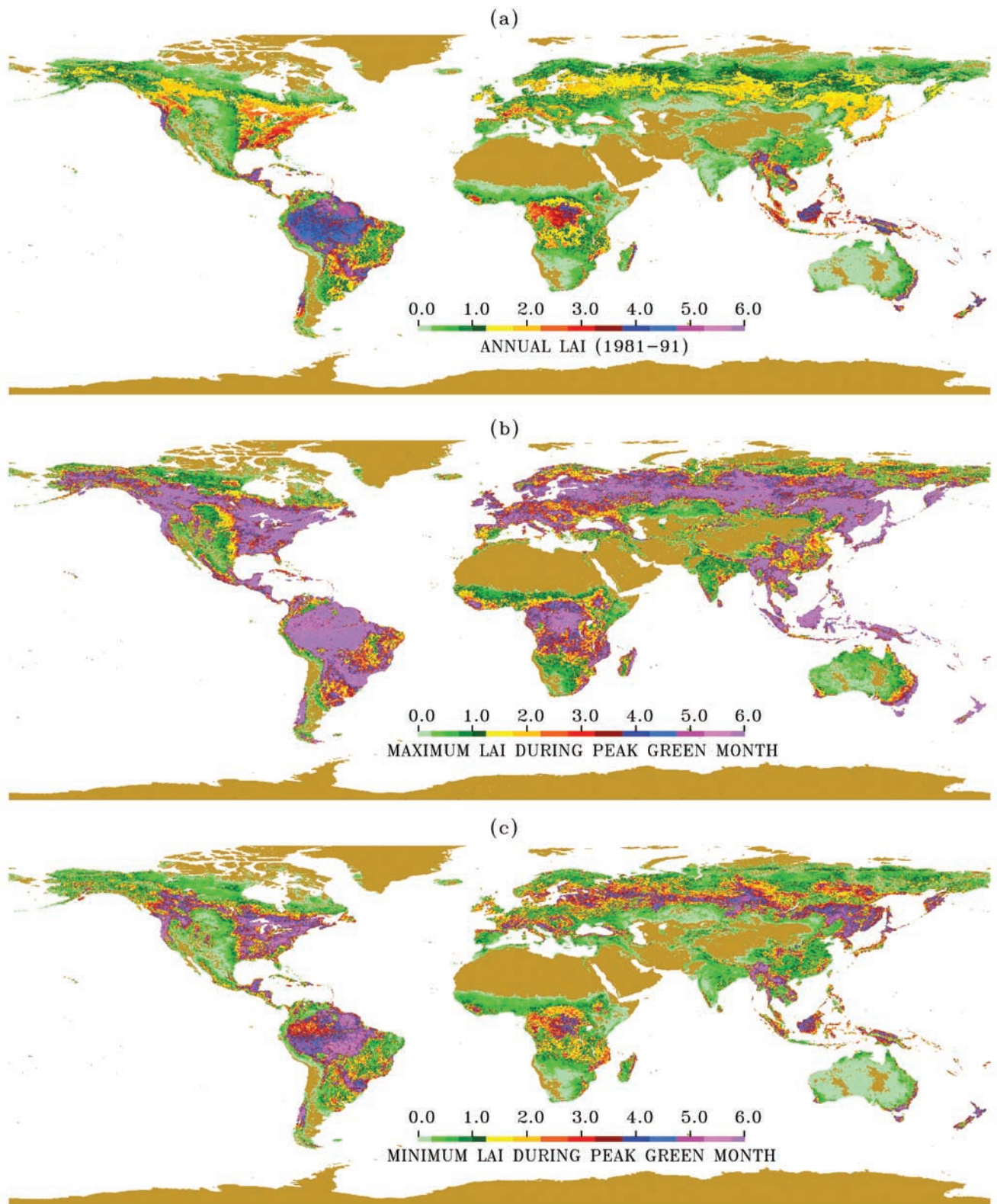


**Figure 7.** Geographical distribution of LAI: (a) the geographical distribution of annual LAI and (b, c) the maximum and minimum LAI over the 1981–1991 period during the month of peak greenness.

The objective here is to identify regions where vegetation growth is generally affected by ENSO events independent of various lags and where variations in LAI are directly related to variations in SSTs. Pixels with 12 month cumulative LAI anomaly greater than 2 or lesser than -2, and those correlated significantly at the 5% level are shown in Figures 8a and 8c. Figures 8b and 8d show the same, but a one month lag in LAI was assumed to account for SST anomalies to propagate their influence.

[33] Monthly LAI anomalies in eastern Australia, northeast Brazil, southeast and central Africa, Indonesia, central America, the west coast of the United States, and to a lesser extent, southeastern United States, and southwestern Europe, correlate negatively with the monthly NINO3 index (decreased LAI) during the warm event of 1982–1983. Only in south-central and southeastern South America and southwestern Africa do LAI anomalies show a positive correlation with the NINO3 index (increased LAI). During the cold event of 1988–1989, monthly LAI anomalies in eastern Australia, northeast Brazil, and to a lesser extent, in central Africa, west coast of the United States, southeastern United States, and southwestern Europe, correlate negatively with the NINO3 index (increased LAI; Figure 8c). Southeastern South America exhibits a large negative LAI anomaly. The spatial patterns of LAI anomalies observed during these two well-defined ENSO events conform to reported patterns in rainfall anomalies [Ropelewski and Halpert, 1987; Dai et al., 1997].

[34] The time series of LAI and rainfall anomalies in regions showing significant correlation between LAI and SST anomalies are shown in Figure 9. There is notable coherence between LAI and rainfall anomalies in these semiarid areas. The negative rainfall and LAI anomalies during the warm event of 1982–1983 can be seen in northeast Brazil, eastern Australia and southeast Africa. The severe and extensive drought of 1988–1989 in southeastern South America associated with the cold event can also be seen. During the cold event, the wet conditions expected in northeast Brazil, eastern Australia, and southeast Africa are discernable in the rainfall time series but are distinct in the LAI anomaly time series. Overall, the observed spatial and temporal agreement between satellite LAI and station rainfall anomalies imbues further confidence in the derived LAI data set.

#### 5.4. LAI Variation and Surface Temperature in the North

[35] An increasing NDVI trend in the northern latitudes during the 1980s was reported previously [Myneni et al., 1997b]. It was speculated that this increased plant growth was possibly due to a warming trend in these regions. Here we present LAI trends for an extended period (1981–1994) and assess their correlation to station temperature data as an exercise to further verify variations in the LAI data set.

[36] The geographical distribution of local changes from 1981 to 1994 in summer time LAI of vegetated areas north of 25°N is shown in Figure 10. Eurasian vegetation in the latitude band between 50°N and 65°N shows the largest increase in LAI, and this includes southern Russia and a broad region in Siberia north of Lake Baikal. Outside this band, significant LAI increase can also be seen in northeastern Mongolia, China and Siberia, northern Fenno-scandia

(Finmark and the Kola peninsula), and west central Europe. In North America, regions of enhanced LAI comprise the three southwestern Canadian provinces (British Columbia, Alberta, Saskatchewan), and some pockets in the midwestern United States. North American vegetation, though, shows considerably less increase in LAI and regions with increasing LAI tend to be more fragmented. For this time period, notable decreases in LAI are seen in southern Scandinavia, the Pacific Northwest, and over regions south of the Hudson Bay and east of the Ural Mountains (West Siberian Plain).

[37] In general, the regions of large LAI increase are north of 50°N and in the interiors of the Eurasian and, to a smaller extent, North American continents. A comparison with the spatial distribution of annual LAI (Figure 7a) indicates that these regions closely coincide with the distribution of needleleaf forests in the boreal and temperate zones. This suggests that the largest LAI increases over this time period happened in areas with already abundant vegetation.

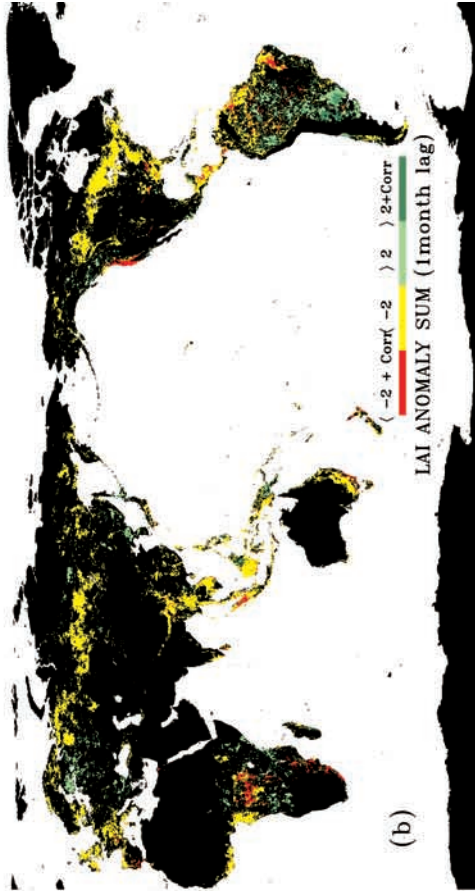
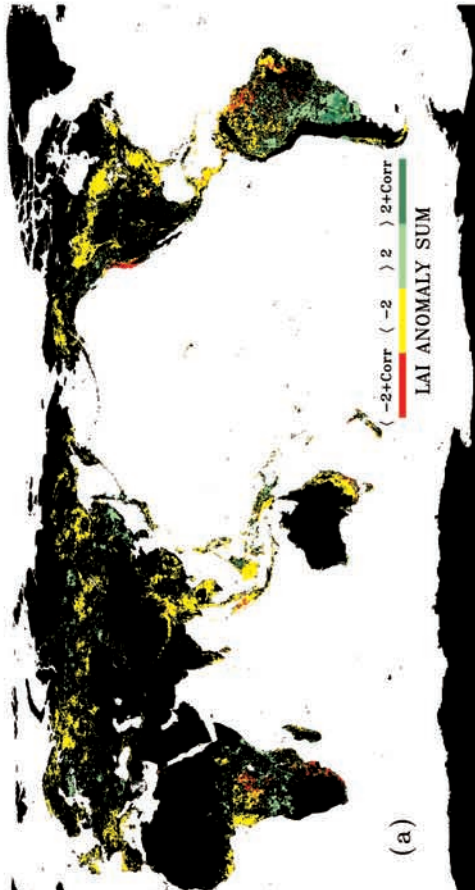
[38] The trends in station temperature and LAI anomalies and their correlation during the spring and summer periods in Eurasia and North America are shown in Figure 11. Variations in spring time near-surface station temperature and satellite based LAI anomalies correlate remarkably well in the northern high latitudes. For Eurasia, the good correlation for the 40°N to 70°N latitude band masks the weak correlation in the corresponding temperate band (40°N to 50°N). In the boreal latitudes (50°N to 70°N), the correlations are significant and the trends are consistent between the two continents. The pronounced Pinatubo cooling in the boreal latitudes during spring 1992 is also well captured in the LAI data [see also Parker et al., 1996]. The summer temperature trends and relations to LAI are considerably weaker. It is interesting to note that the significant trend in summer time LAI anomalies over Eurasian temperate and boreal latitudes shows little direct correlation to summer temperature anomalies. This enhanced plant growth might in part be associated with warmer temperatures in the spring and an associated lengthening of the active growing season [Myneni et al., 1997b].

[39] These relations suggest that warmer temperatures may have promoted plant growth in the north during the time period 1981–1994, but this simplistic explanation may be valid only at coarse spatial scales. Possibly it is not mechanistically viable for all northern ecosystems and needs to be refined to allow for lags in the relation between plant growth and temperature induced by biogeochemical feedbacks [Braswell et al., 1997; Houghton et al., 1998; Potter and Klooster, 1999]. Moreover, the record length (13–14 years) is too short for rigorous trend analysis. However, recent results from an extended NDVI data set (1981–1999) provide evidence that the observed trends in vegetation growth are robust [Zhou et al., 2001].

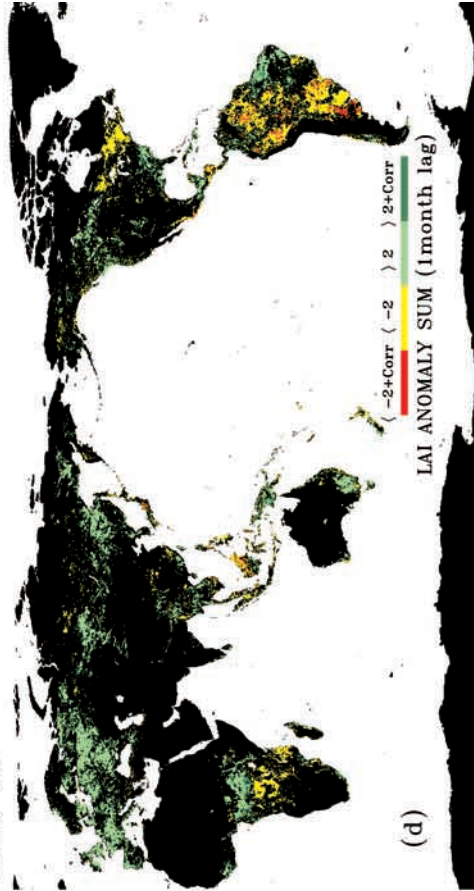
## 6. Conclusions

[40] A global data set of monthly leaf area index (LAI) derived from satellite NDVI observations for the period July 1981 to September 1994 is discussed in this article. Validation of the derived LAI fields is a challenging task, yet without this, the utility of the data set will be limited. By

EL NINO 1982-83



LA NINA 1988-89



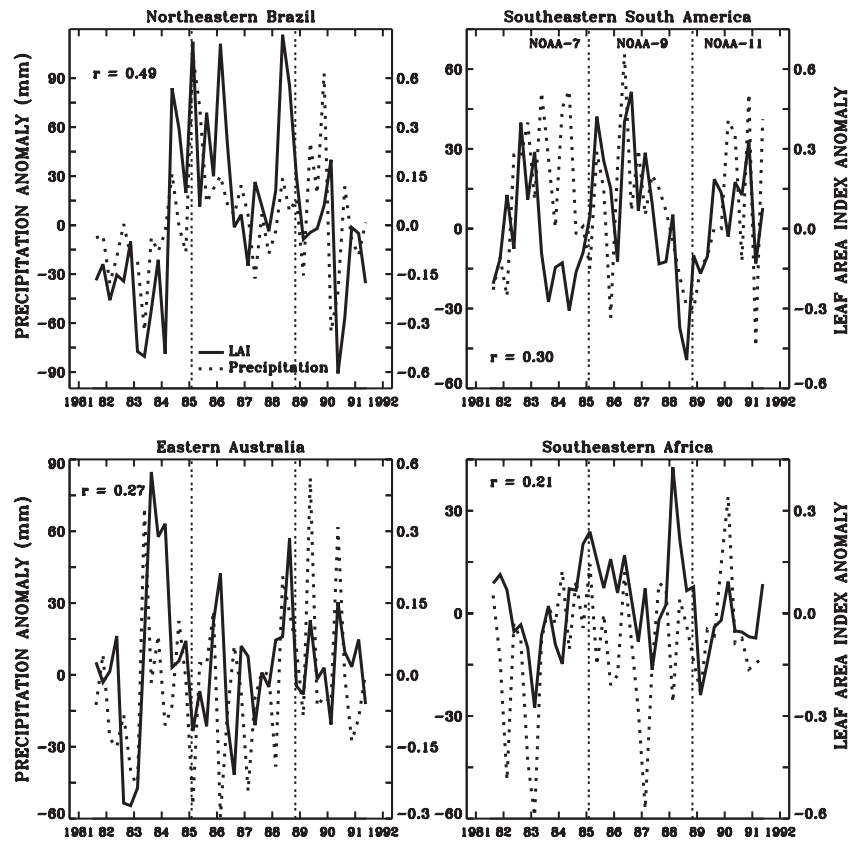


**Figure 9.** Time series of LAI (solid line) and rainfall (dotted line) anomalies in ENSO affected regions. The rainfall data are from *Dai et al.* [1997], and the anomalies are with respect to the 1951–1979 mean. The anomaly plots are three month averages. The rainfall (2.5° resolution) and LAI (0.25° resolution) anomalies were spatially averaged for northeastern Brazil (3°S–12°S, 36°W–43°W), southeastern South America (25°S–35°S, 49°W–60°W), eastern Australia (20°S–38°S, 146°E–154°E), and southeastern Africa (20°S–25°S, 29°E–34°E). The significance levels for correlations with 40 observations are  $r = 0.31$  (5% level) and  $r = 0.21$  (10% level), respectively.

validation we mean the specification of uncertainties in the derived fields with respect to ground measurements. The retroactive nature of this coarse resolution (8 km) global multiyear data set demands repetitive ground measurements from all representative vegetation types for validation, but such observations are not available. Nevertheless, we have tried to assess the magnitudes and interannual variations in the LAI fields through five different activities.

[41] First, we estimated the magnitude of errors incurred by the use of the NDVI-based algorithm as opposed to a more physically based approach. This analysis indicated that the relative error in LAI is about 10–20% in dense biomes, for example forests, which is approximately comparable to the estimated mean uncertainty of input AVHRR channel data from which NDVI was computed. Second,

ground measurements of LAI from three campaigns were used to verify the magnitude of the produced fields. The results suggested that the magnitude of satellite LAI values are comparable to field observations, at sites representative of grasses and needleleaf forest biomes. Third, the data set was compared to another LAI data set currently used by the community. This exercise indicated good qualitative agreement with respect to interannual variability. However, the LAI values of the earlier data were consistently larger than those derived here. Fourth, through correlations with climate data sets, e.g., land and sea surface temperatures and precipitation, we argued for meaningful interannual variations observed in our LAI data set. The spatial and temporal agreement between satellite LAI and station rainfall anomalies in tropical semiarid regions affected by the ENSO

**Figure 8.** (opposite) Geographical distribution of cumulative monthly LAI anomaly (a,b) from May 1982 to April 1983 and from (c,d) May 1988 to April 1989. The association between monthly sea surface temperature anomaly (NINO3) [Reynolds and Smith, 1994] and monthly LAI anomaly during the respective 12 month ENSO cycle was determined through correlation analysis (b, d represent one month LAI lag correlations). Areas with cumulative monthly LAI anomaly greater than 2 or lower than -2 and correlated significantly at the 5% level ( $r > 0.58$ ;  $f$  statistic) were contoured.

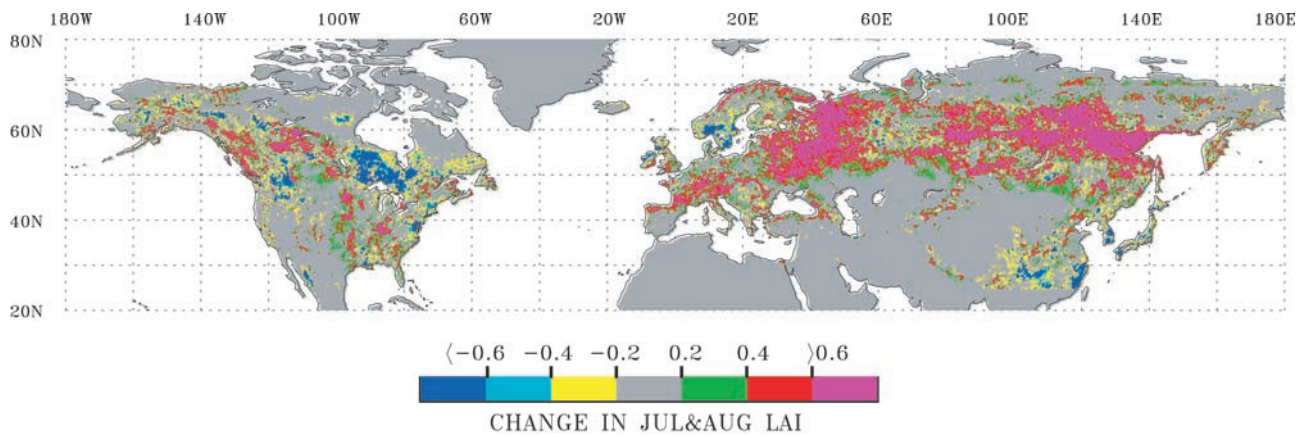


**Figure 10.** Geographical distribution of local changes from 1981 to 1994 in LAI of vegetated areas north of 25°N, expressed as the average of July and August LAI. The increase over 14 years was determined by linear regression of year-to-year LAI.

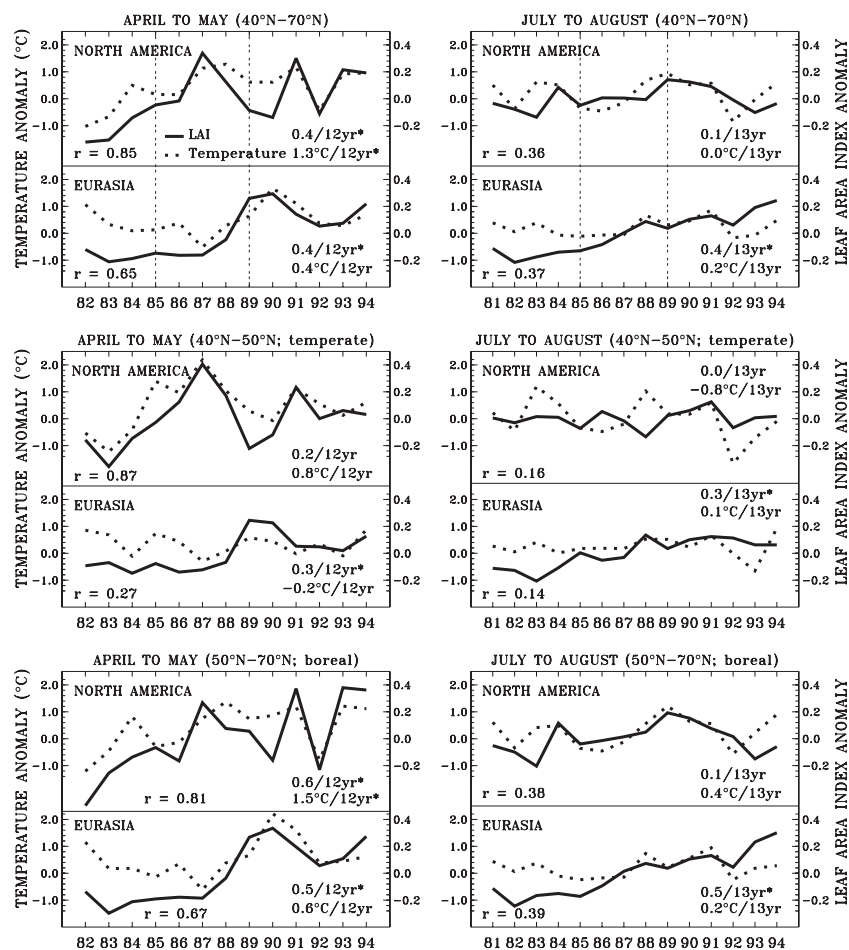


**Figure 11.** Trends in LAI (solid line) and station temperature anomalies (dotted line) and their correlation (linear Pearson) during the spring (April–May) and summer periods (July August) over vegetated areas in Eurasia and North America. The bi-monthly LAI anomalies for spring/summer are relative to the period 1982–1994/1981–1994, respectively. The bimonthly temperature anomalies (2.0° resolution) are based on the 1951–1980 mean [Hansen *et al.*, 1999]. Trends (see insets) were determined through linear regression. Values with a star represent trends that are statistically significant at the 10% level (*t* statistic). Also note that the correlation significance levels for 13/14 observations are 0.48/0.46 (10% level) and 0.55/0.53 (5% level), respectively. Changes of satellite platforms are indicated in the top two graphs (dashed-dotted line).

phenomenon further imbues confidence in the LAI data set. A similar exercise where the LAI variations in northern vegetation were correlated to station temperature data argues for consistency between satellite data retrievals and ground measurements. Finally, the value of the data set is documented through climate model simulations with the satellite LAI fields that improved model simulation of near-surface climate. This is reported by *Buermann et al.* [2001]. While these activities do not constitute comprehensive validation per se, they at the very least argue for utility of this data set for global scale modeling studies. The data set is available to the community via our Web server (<http://cybele.bu.edu>).

[42] **Acknowledgments.** We thank the International Research Institute (IRI) Data Library, Lamont-Doherty Earth Observatory of Columbia University, Palisades, New York, for making SST (NINO3 index) data available. Further, we thank the Distributed Active Archive Center (DAAC), hosted at the Oak Ridge National Laboratory, for providing all the LAI field observations from large-scale field campaigns. This research was funded by the NASA Earth Science Enterprise and NOAA Office of Global Programs.

## References

- Asrar, G., M. Fuchs, E. T. Kanemasu, and J. L. Harfield, Estimating absorbed photosynthetic radiation and leaf area index from spectral reflectance in wheat, *Agron. J.*, **76**, 300–306, 1984.
- Berthelot, B., S. Adam, L. Kergoat, F. Cabot, G. Dedieu, and P. Maison-grande, A global data set of surface reflectances and vegetation indices derived from AVHRR/GVI time series for 1989 and 1990: The LAnd Surface Reflectances (LASUR) data, paper presented at the Seventh International Symposium on Physical Measurements and Signatures in Remote Sensing, Int. Soc. for Photogramm. and Remote Sens., Courchevel, France, 7–11 April, 1997.
- Braswell, B. H., D. S. Schimel, E. Linder, and B. Moore, The response of global terrestrial ecosystems to interannual temperature variability, *Science*, **238**, 870–872, 1997.
- Buermann, W., J. Dong, X. Zeng, R. B. Myneni, and R. E. Dickinson, Evaluation of the utility of satellite based vegetation leaf area index data for climate simulations, *J. Clim.*, **14**, 3536–3550, 2001.
- Chen, J. M., and J. Cihlar, Retrieving leaf area index of boreal conifer forests using Landsat TM images, *Remote Sens. Environ.*, **55**, 153–162, 1996.
- Cowan, P. R., Stomatal behavior and environment, *Adv. Bot. Res.*, **4**, 117–128, 1977.
- Dai, A., and T. M. L. Wigley, Global patterns of ENSO-induced precipitation, *Geophys. Res. Lett.*, **27**, 1283–1286, 2000.
- Dai, A., I. Y. Fung, and A. D. Del Genio, Surface observed global land precipitation variations during 1900–88, *J. Clim.*, **10**, 2943–2962, 1997.
- Dickinson, R. E., Modeling evapotranspiration for three-dimensional global climate models, in *Climate Processes and Climate Sensitivity*, *Geophys. Monogr. Ser.*, vol. 29, edited by J. E. Hanson and T. Takahashi, pp. 58–72, AGU, Washington, D. C., 1984.
- Dickinson, R. E., Land-atmosphere interaction, *U.S. Natl. Rep. Int. Union Geod. Geophys. 1991–1994, Rev. Geophys.*, **33**, 917–922, 1995.
- Field, C. B., and H. A. Mooney, *On the Economy of Plant Form and Function*, edited by T. J. Givnish, pp. 22–55, Cambridge Univ. Press, New York, 1986.
- Gobron, N., B. Pinty, and M. M. Verstraete, Theoretical limits to the estimation of the Leaf Area Index on the basis of visible and near-infrared remote sensing data, *IEEE Trans. Geosci. Remote Sens.*, **35**, 1438–1445, 1997.
- Hansen, J., R. Ruedy, J. Glascoe, and M. Sato, GISS analysis of surface temperature change, *J. Geophys. Res.*, **104**, 30,997–31,022, 1999.
- Houghton, R. A., E. A. Davidson, and G. M. Woodwell, Missing sinks, feedbacks, and understanding the role of terrestrial ecosystems in the global carbon balance, *Global Biogeochem. Cycles*, **2**, 25–34, 1998.
- James, M. E., and S. N. V. Kalluri, The Pathfinder AVHRR land data set: An improved coarse-resolution data set for terrestrial monitoring, *Int. J. Remote Sens.*, **15**, 3347–3364, 1994.
- Knyazikhin, Y., J. V. Martonchik, R. B. Myneni, D. J. Diner, and S. W. Running, Synergistic algorithm for estimating vegetation canopy leaf area index and fraction of absorbed photosynthetically active radiation from MODIS and MISR data, *J. Geophys. Res.*, **103**, 32,257–32,276, 1998a.
- Knyazikhin, Y., J. V. Martonchik, D. J. Diner, R. B. Myneni, M. M. Verstraete, B. Pinty, and N. Gobron, Estimation of vegetation canopy leaf area index and fraction of absorbed photosynthetically active radiation from atmosphere-corrected MISR data, *J. Geophys. Res.*, **103**, 32,239–32,256, 1998b.
- Los, S. O., C. O. Justice, and C. J. Tucker, A global 1 by 1 NDVI data set for climate studies derived from the GIMMS continental NDVI data, *Int. J. Remote Sens.*, **15**, 3493–3518, 1994.
- Los, S. O., G. J. Collatz, P. J. Sellers, C. M. Malmstroem, N. H. Pollack, R. S. DeFries, L. Bounoua, M. T. Parriss, C. J. Tucker, and D. A. Dazlich, A global 9-year biophysical land surface data set from NOAA AVHRR data, *J. Hydrometeorol.*, **1**, 183–199, 2000.
- McBride, J. L., and N. Nicholls, Seasonal relationships between Australian rainfall and the Southern Oscillation, *Mon. Weather Rev.*, **111**, 1998–2004, 1983.
- Miller, J. R., H. P. White, and J. M. Chen, Seasonal change in understory reflectance of boreal forests and influence on canopy vegetation indices, *J. Geophys. Res.*, **102**, 29,475–29,482, 1997.
- Myneni, R. B., S. O. Los, and C. J. Tucker, Satellitebased identification of linked vegetation index and sea surface temperature anomaly areas from 1982–1990 for Africa, Australia and South America, *Geophys. Res. Lett.*, **23**, 729–732, 1996.
- Myneni, R. B., R. R. Nemani, and S. W. Running, Estimation of global leaf area index and absorbed par using radiative transfer models, *IEEE Trans. Geosci. Remote Sens.*, **35**, 1380–1393, 1997a.
- Myneni, R. B., C. D. Keeling, C. J. Tucker, G. Asrar, and R. R. Nemani, Increased plant growth in the northern high latitudes from 1981 to 1991, *Nature*, **386**, 698–702, 1997b.
- Myneni, R. B., C. J. Tucker, G. Asrar, and C. D. Keeling, Interannual variations in satellite-sensed vegetation index data from 1981 to 1991, *J. Geophys. Res.*, **103**, 6145–6160, 1998.
- Myneni, R. B., et al., Global products of vegetation leaf area and fraction absorbed PAR from year one of MODIS data, *Remote Sens. Environ.*, in press, 2002.
- Nelson, A., J. Killeen, L. Ballou, T. Shah, and C. Hays, First ISLSCP Field Experiment Biophysical Properties of Vegetation Data Set, in *The First ISLSCP Field Experiment*, vol. 1, *Surface Observations and Non-Image Data Sets* [CD-ROM], edited by D. E. Strelbel, D. R. Landis, K. F. Huemmrich, and B. W. Meeson, NASA, Washington, D. C., 1994. (Available at <http://www-eosdis.ornl.gov>)
- Parker, D. E., H. Wilson, P. D. Jones, J. R. Christy, and C. K. Folland, The impact of Mount Pinatubo on worldwide temperatures, *Int. J. Climatol.*, **16**, 487–497, 1996.
- Peterson, D. L., M. A. Spanner, S. W. Running, and L. Band, Relationship of Thematic Mapper Simulator data to leaf area index, *Remote Sens. Environ.*, **22**, 323–341, 1987.
- Potter, C. S., and S. A. Klooster, Detecting a terrestrial biosphere sink for carbon dioxide: Interannual ecosystem modeling for the mid-1980s, *Clim. Change*, **42**, 489–503, 1999.
- Potter, C. S., J. T. Randerson, C. B. Field, P. A. Matson, P. M. Vitousek, H. A. Mooney, and S. A. Klooster, Terrestrial Ecosystem Production, a process model, based on global satellite and surface data, *Global Biogeochem. Cycles*, **7**, 811–841, 1993.
- Reynolds, R. W., and T. M. Smith, Improved global sea surface temperature analyses using optimum interpolation, *J. Clim.*, **7**, 929–948, 1994.
- Ropelewski, C. F., and M. S. Halpert, Global and regional scale precipitation pattern associated with the El Niño/Southern Oscillation, *Mon. Weather Rev.*, **115**, 1606–1626, 1987.
- Ropelewski, C. F., and M. S. Halpert, Precipitation patterns associated with the high index phase of the Southern Oscillation, *J. Clim.*, **2**, 268–284, 1989.
- Sellers, P. J., S. O. Los, C. J. Tucker, C. O. Justice, D. A. Dazlich, G. J. Collatz, and D. A. Randall, A revised land surface parameterization (SIB-2) for atmospheric GCMs, part 2, The generation of global fields of terrestrial biophysical parameters from satellite data, *J. Clim.*, **9**, 706–737, 1996.
- Sellers, P. J., et al., Modeling the exchanges of energy, water, and carbon between continents and the atmosphere, *Science*, **275**, 502–509, 1997a.
- Sellers, P. J., et al., BOREAS in 1997: Experiment overview, scientific results, and future directions, *J. Geophys. Res.*, **102**, 28,731–28,769, 1997b.
- Steyaert, L. T., F. G. Hall, and T. R. Loveland, Land cover mapping, fire generation, and scaling studies in the Canadian boreal forest with 1 km AVHRR and Landsat TM data, *J. Geophys. Res.*, **102**, 29,581–29,598, 1997.
- Tian, Y., Y. Zhang, Y. Knyazikhin, R. B. Myneni, J. Glassy, G. Dedieu, and S. W. Running, Prototyping of MODIS LAI and FPAR algorithm with LASUR and LANDSAT data, *IEEE Trans. Geosci. Remote Sens.*, **38**, 2387–2401, 2000.
- Tian, Y., Y. Wang, Y. Zhang, Y. Knyazikhin, J. Bogaert, and R. B. Myneni, Radiative transfer based scaling of LAI/FPAR retrievals from re-

- flectance data of different resolutions, *Remote Sens. Environ.*, in press, 2002.
- Tucker, C. J., I. Y. Fung, C. D. Keeling, and R. H. Gammon, Relationship between atmospheric CO<sub>2</sub> variations and a satellite-derived vegetation index, *Nature*, 319, 195–199, 1986.
- Ustin, S. L., Oregon Transect Ecosystem Research, Leaf Area Index Data data set, in *OTTER Pilot Land Data System*, vol. 1, version 1, *Satellite, Aircraft and Ground Measurements* [CD-ROM], edited by G. L. Angelici, J. W. Skiles, and L. Z. Popovici, NASA, 1990. (Available at <http://www-eosdis.ornl.gov>)
- Vautard, R., P. Yiou, and M. Ghil, Singular-spectrum analysis: A toolkit for short, noisy chaotic signals, *Phys. D*, 58, 95–126, 1992.
- Wang, Y., Y. Tian, Y. Zhang, N. El-Saleous, Y. Knyazikhin, E. Vermote, and R. B. Myneni, Investigation of product accuracy as a function of input and model uncertainties: Case study with SeaWiFS and MODIS LAI/FPAR algorithm, *Remote Sens. Environ.*, 78, 296–311, 2001.
- Zhou, L., C. J. Tucker, R. K. Kaufmann, D. Slayback, N. V. Shabanov, and R. B. Myneni, Variations in northern vegetation activity inferred from satellite data of vegetation index during 1981–1999, *J. Geophys. Res.*, 106, 20,069–20,083, 2001.
- 
- W. Buermann, J. Dong, R. B. Myneni, Y. Wang, and L. Zhou, Department of Geography, Boston University, 675 Commonwealth Avenue, Boston, MA 02215, USA. ([buerman@bu.edu](mailto:buerman@bu.edu))
- R. E. Dickinson, School of Earth and Atmospheric Sciences, Georgia Institute of Technology, Atlanta, GA 30332, USA.
- C. S. Potter, Ecosystem Science and Technology Branch, NASA Ames Research Center, Moffet Field, CA 94035, USA.
- X. Zeng, Institute of Atmospheric Physics, University of Arizona, Tucson, AZ 85721, USA.